DOI: 10.1002/ejic.201101361

Water-Soluble Copper(II) Complexes with a Sulfonic-Functionalized Arylhydrazone of β-Diketone and Their Application in Peroxidative Allylic Oxidation of Cyclohexene

Archana Mizar,[a] M. Fátima C. Guedes da Silva,*[a,b] Maximilian N. Kopylovich,[a] Sanghamitra Mukherjee,[a] Kamran T. Mahmudov,[a,c] and Armando J. L. Pombeiro*[a]

Keywords: Hydrazones / Ketones / Copper / Structure elucidation / Oxidation

The reaction of Cu^{II} acetate with the new sulfo-functionalized arylhydrazone of β-diketone 2-[2-(4,4-dimethyl-2,6-dioxocyclohexylidene)hydrazinyl]benzenesulfonic acid (H_2L, **1**) in aqueous methanol solution led to the formation of the 2D coordination polymer $\{[Cu_4(1\kappa^2O,\kappa N{:}2\kappa O,\kappa N\text{-}L)_4(\mu\text{-}OH_2)_2]\cdot H_2O\}_n$ (**2**). However, when the reaction was peformed in the presence of the N-containing species cyanoguanidine (cyg), 3,5-dimethyl-1*H*-pyrazole (dp), 2,2′-bipyridine (bpy) or pyrazine (py), the mononuclear $(H_3O^+)_2[Cu(\kappa^2O,\kappa N\text{-}L)_2]$ (**4**), $[Cu(\kappa^2O,\kappa N\text{-}L)(dp)_2]$ (**3**) or $[Cu(\kappa^2O,\kappa N\text{-}L)(\kappa^2N\text{-}bpy)]$ (**5**) or dinuclear $[\{Cu(\kappa^2O,\kappa N\text{-}L)(H_2O)\}_2(\kappa\text{-}py)]\cdot CH_3OH$ (**6**) complexes were obtained, respectively. The compounds were characterized by elemental analysis, IR spectroscopy, single-crystal X-ray diffraction analysis and, for **1**, by ^1H and ^{13}C NMR spectroscopy. The Cu^{II} complexes **2**–**6** act as catalyst precursors for the selective peroxidative (with TBHP) allylic oxidation of cyclohexene to cyclohex-2-enol (Cy-ol) and cyclohex-2-enone (Cy-one), formed in a Cy-one/Cy-ol ratio of up to 9 with total yields of around 70 % and TONs of up to 350.

Introduction

Arylhydrazones of β-diketones (hereafter denoted as AHBDs) and their complexes have attracted considerable attention due to their high synthetic potential in organic[1] and inorganic[2] chemistry and their wide range of useful properties. For example, AHBDs can find applications in the design of functional materials attributed to smart hydrogen bonding,[3] photo-triggered structural switching,[4a] self-assembled layers,[4b] liquid crystals,[4c] semiconductors,[4d,4e] ionophores,[4f] indicators,[4g] spectrophotometric reagents for the determination of metal ions,[4h,4i] catalysts,[2a,4j–4l] photoluminescent materials,[4m] optical recording media[4n] and spin-coating films.[4o]

The water solubility of the AHBD compounds has particular importance for catalysis and other applications in which water is used as solvent and/or reactant. For instance, we have previously shown[5] that water-soluble Cu^{II}–AHBD complexes are suitable catalysts for the TEMPO-mediated aerobic oxidation of benzylic alcohols in aqueous media. Incorporation of a hydrophilic polar (e.g., sulfo or arseno) group into the ligand is one of the common ways to increase the water solubility of its complexes. Moreover, such a ligand can behave as a polydentate donor moiety, thus supporting an extension of coordination arrays in the solid state. In addition, it has been noted[4k] that particularly stable complexes with two fused six-membered metallacycles can be synthesized by taking advantage of the coordination ability of an *ortho* substituent of the AHBD.

The use of a hetero-proligand (e.g. imidazole, cyanoguanidine, ethylenediamine) in a Cu^{II}–AHBD can modulate, to some extent, the structure of the thus synthesized complexes.[4k] The auxiliary species affects the complexation process through coordination, template condensation or as a proton attractor or spacer, thus allowing regulation of the structures of the primary subunits as well as their supramolecular assemblies.[6] Hence, AHBDs and their complexes can form interesting architectures involving monomeric, oligomeric or polymeric subunits.[2,4k] This structure modulation is related to current topics of crystal engineering[7a] and molecular recognition[7b,7c] aiming at the design of materials that may be used for compound storage[7d,7e] or chemical sensing.[7f]

On the other hand, it has been shown[2a,4k,5] that Cu^{II}–AHBD complexes are valuable catalysts for some oxidation processes, for example, the peroxidative oxidation reactions of cyclohexane and alcohol. Moreover, the selective allylic oxidation of alkenes, which preserves the C=C double bond

---

[a] Centro de Química Estrutural, Complexo I, Instituto Superior Técnico, Technical University of Lisbon,
Av. Rovisco Pais, 1049-001 Lisbon, Portugal
E-mail: pombeiro@ist.utl.pt
[b] Universidade Lusófona de Humanidades e Tecnologias, ULHT Lisbon,
Campo Grande 376, 1749-024 Lisboa, Portugal
E-mail: fatima.guedes@ist.utl.pt
[c] Baku State University, Department of Chemistry,
Z. Xalilov Str. 23, Az 1148 Baku, Azerbaijan

Supporting information for this article is available on the WWW under http://dx.doi.org/10.1002/ejic.201101361.

and allows further functionalization, is a very useful synthetic transformation that deserves further investigation to find new effective catalysts. Some copper complexes have been found to catalyse such reactions,[8] but so far there have been no report of the use of Cu^{II}–AHBD catalysts for this purpose. Hence, it is worthwhile attempting to use Cu^{II}–AHBD complexes as catalysts for this selective transformation under mild conditions. The oxidation of cyclohexene to cyclohex-2-enol and cyclohex-2-enone with *tert*-butyl hydroperoxide (TBHP) (Scheme 1) was chosen as a model reaction.

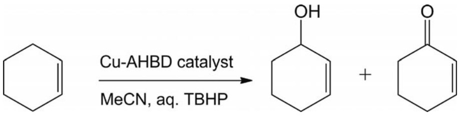

Scheme 1.

Thus, in this work we combine the above-mentioned approaches to achieve our aims: 1) the synthesis of a new water-soluble AHBD species bearing a sulfonic group, 2-[2-(4,4-dimethyl-2,6-dioxocyclohexylidene)hydrazinyl]benzenesulfonic acid (H_2L, **1**), which contains an *ortho*-SO_3H moiety, and its application to the preparation of new water-soluble Cu^{II}–AHBD complexes, 2) the design of diverse Cu^{II}–AHBD hetero-ligand-containing complexes of different geometries and nuclearities and 3) the use of these complexes as catalysts or catalyst precursors for the selective peroxidative allylic oxidation of cyclohexene to cyclohex-2-enol and cyclohex-2-enone.

Results and Discussion

Synthesis and Characterization of 1 and Its Copper(II) Complexes

The water-soluble AHBD **1** (Scheme 2) was synthesized by a modified Japp–Klingemann reaction:[9a–9c] 2-sulfophenyldiazonium chloride was treated with 5,5-dimethylcyclohexane-1,3-dione in an ethanolic solution of sodium hydroxide.[9d] 2-Sulfophenyldiazonium chloride was obtained by diazotization of the corresponding substituted aniline. AHBD **1** is highly soluble in polar solvents such as water, DMF and DMSO, but almost insoluble in chloroform, dichloromethane and toluene. The presence of the SO_3H group is crucial for its solubility in water; the unfunctionalized analogue of **1**, with H instead of SO_3H, is insoluble in water.[2a,4k]

The NMR spectrum of **1** in [D6]DMSO at room temperature indicates that this compound exists in this solvent in the hydrazone rather than the enol-azo or keto-azo form.[2] The two resonances in the ^{13}C NMR spectrum arising from the carbonyl groups (see the Exp. Sect.) show that one of these groups undergoes a shift due to hydrogen

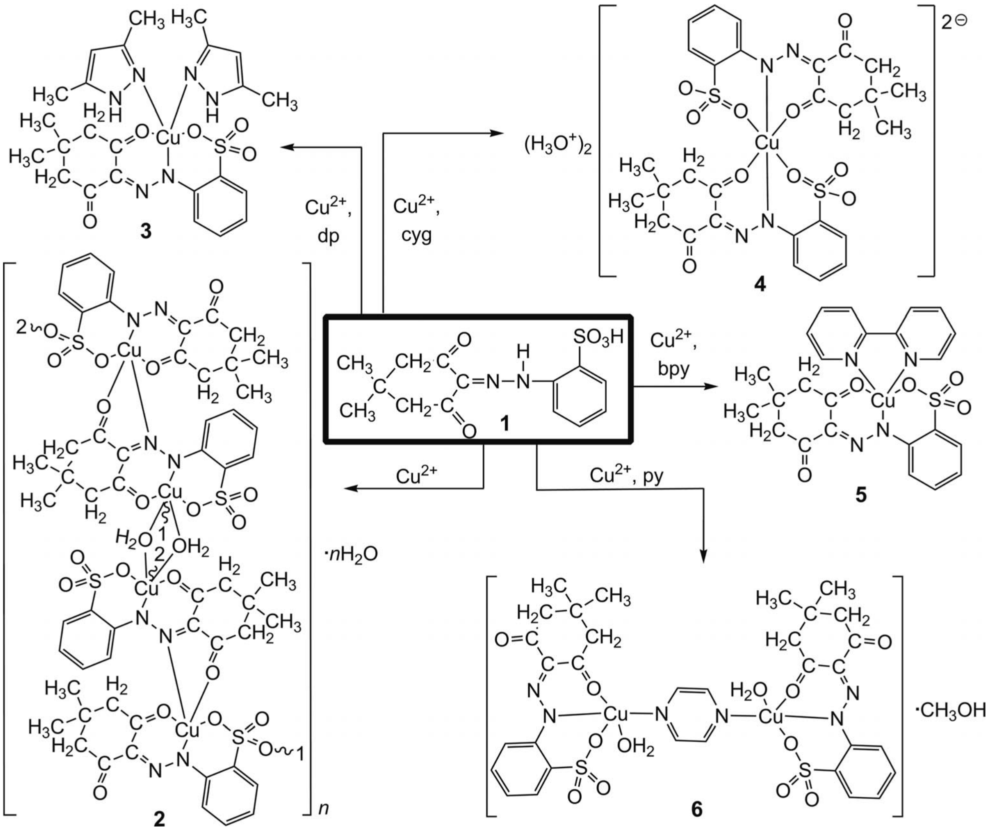

Scheme 2. Reactions of Cu^{II} acetate with **1** in water in the presence and absence of auxiliary ligands (a H_2O/CH_3OH mixture was used as solvent for the recrystallization).

bonding with the hydrazone NH moiety. This is in accord with the low-field ^{1}H chemical shift (δ = 15.28 ppm) of the hydrazone NH proton and is also consistent with the IR data: IR bands for ν(C=O) and ν(C=O···H) appear at 1664 and 1630 cm^{-1}, respectively, the latter being shifted on account of the hydrogen bond.[2–5] The ν(OH) and ν(NH) bands at 3491 and 2954 cm^{-1}, respectively, also support[2–5] the existence of the hydrogen-bonded hydrazone structure in the solid state. Moreover, the single-crystal X-ray analysis of **1** (Figure 1) also shows that, in the solid phase, it exists in the hydrazone form, although with electron delocalization. The N1–N2 bond length of 1.255(6) Å is typical of a double bond, whereas that of C6–N1 [1.421(7) Å] is representative of a C_{Ar}–NH–N= moiety. However, the C7–N2 bond length of 1.324(7) Å is close to the value of a classic C_{sp^2}–N bond (1.336 Å),[10] thus providing evidence for electron delocalization over the OCCCO skeleton. Thus, the C–O bond lengths of 1.238(6) and 1.240(6) Å are close to those usually found in delocalized double bonds in carboxylate anions.[10] Such delocalization is also the reason for the weak π_{OCCCO}···H14C interaction (centroid···H and ∠ centroid···H14C–C14, 3.290 Å and 168.77°, respectively). There are intramolecular hydrogen bonds in **1** (see Figure 1) that strengthen the hydrazone form of the molecule and influence its coplanarity. Indeed, molecule **1** is nearly planar, as indicated by the very low angle (5.87°) between the $C_{C=O}$–C–$C_{C=O}$-containing plane (hereafter denoted as plane C) and the plane of the aromatic ring (hereafter denoted as plane Ar). This parameter was selected as a way of comparing the degree of coplanarity of molecule **1** and its ligating forms (see below and Table 1).

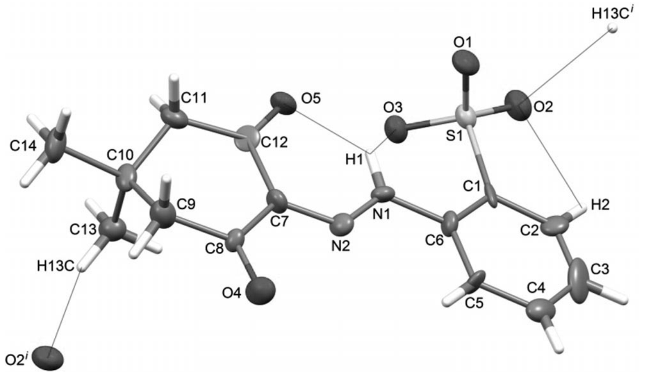

Figure 1. Molecular structure of **1** with atomic numbering scheme and showing the intra- as well as the strongest intermolecular hydrogen-bonding interactions. Thermal ellipsoids are drawn at the 50% probability level. Selected bond lengths [Å] and angles [°]: N1–N2 1.255(6), C6–N1 1.421(7), C7–N2 1.324(7), C12–O5 1.240(6), C8–O4 1.238(6), C7–C8 1.490(6), C7–C12 1.463(8); N2–N1–C6 121.2(4), N1–N2–C7 121.5(5), C1–C6–N1 120.8(5). Selected hydrogen bonds {*d*(H···A) [Å], ∠(DHA) [°]}: N1–H1···O3 2.47, 120.9; N1–H1···O5 1.91, 133.3; C2–H2···O2 2.871(7), 106; C13–H13C···O2 3.461(7), 150. Symmetry operation to generate equivalent atoms: (i) 1.5 – *x*, –*y*, –½ + *z*.

The reaction of $Cu(CH_3COO)_2·H_2O$ with **1** in water/methanol in the absence or in the presence of 3,5-dimethyl-1*H*-pyrazole (dp), cyanoguanidine (cyg), 2,2′-bipyridine (bpy) or pyrazine (py) led to the Cu^{II} complexes {[Cu$_4$(1κ^2*O*,κ*N*:2κ*O*,κ*N*-L)$_4$(μ-OH$_2$)$_2$]·H$_2$O}$_n$ (**2**), [Cu(κ^2*O*,κ*N*-L)(dp)$_2$] (**3**), (H$_3$O$^+$)$_2$[Cu(κ^2*O*,κ*N*-L)$_2$] (**4**), [Cu(κ^2*O*,κ*N*-L)(κ^{2}N-bpy)] (**5**) and [{Cu(κ^2*O*,κ*N*-L)(H$_2$O)}$_2$(κ-py)]·

Table 1. Comparison of selected features of compound **1** and complexes **2**–**6**.

	1	2	3	4	5	6
Organic moiety H$_2$L (or L^{2-})						
N–N [Å]	1.255(6)	1.283(4) 1.295(4)	1.283(9) | 1.375(9)	1.275(3) 1.280(3)	1.283(6)	1.2810(18)
∠ plane C–plane Ar [°][a]	5.87	66.52(18) (Cu1) 21.3(3) (Cu2)	59.6(5) (Cu1) 61.5(5) (Cu2)	39.2(3) (Cu1) 44.19(19) (Cu2)	34.7(3)	57.4(1)
Surrounding of the copper atom						
Cu–N [Å]	–	1.950(3) | 2.448(3)	1.943(8) | 2.092(8)	1.952(2) 1.968(2)	1.980(4) | 2.037(4)	1.9767(13) 2.0235(13)
Cu–O [Å]	–	1.908(2) | 2.342(2)	1.966(6) | 2.140(6)	1.9486(19) | 2.421(2)	1.943(4) 2.255(4)	1.9240(11) | 2.1690(14)
∠ O–Cu–X (X = O or N) [°] Largest Smallest	–	172.46(11) (Cu1) 73.89(10) (Cu2)	174.3(3) (Cu2) 86.7(3) (Cu2)	180.0 82.67(8) (Cu1)	172.1(2) 81.60(18)	171.22(5) 87.55(5)
τ parameter for five-coordinated Cu centre (τ_5)[11]		0.08 (Cu2)	0.67 (Cu1) 0.63 (Cu2)	–	0.21	0.07
Geometry	–	octahedral (Cu1) square pyramidal (Cu2)	trigonal bipyramidal	octahedral	square pyramidal	square pyramidal

[a] For identification of these planes, see text.

CH_3OH (**6**; Scheme 2), which were isolated and characterized by elemental analysis, IR spectroscopy and single-crystal X-ray diffraction.

The reaction of Cu^{II} acetate hydrate with **1** in water afforded a polymer with a tetranuclear core $\{[Cu_4(1\kappa^2O,\kappa N{:}2\kappa O,\kappa N\text{-}L)_4(\mu\text{-}OH_2)_2]\cdot H_2O\}_n$ (**2**; see Figure 2 and Supporting Information, Figure S1), which crystallized directly from the reaction mixture as greenish-black crystals. The polymeric structure of **2** contains crystallographically imposed inversion centres in the heart of the Cu_2O_2 planes.

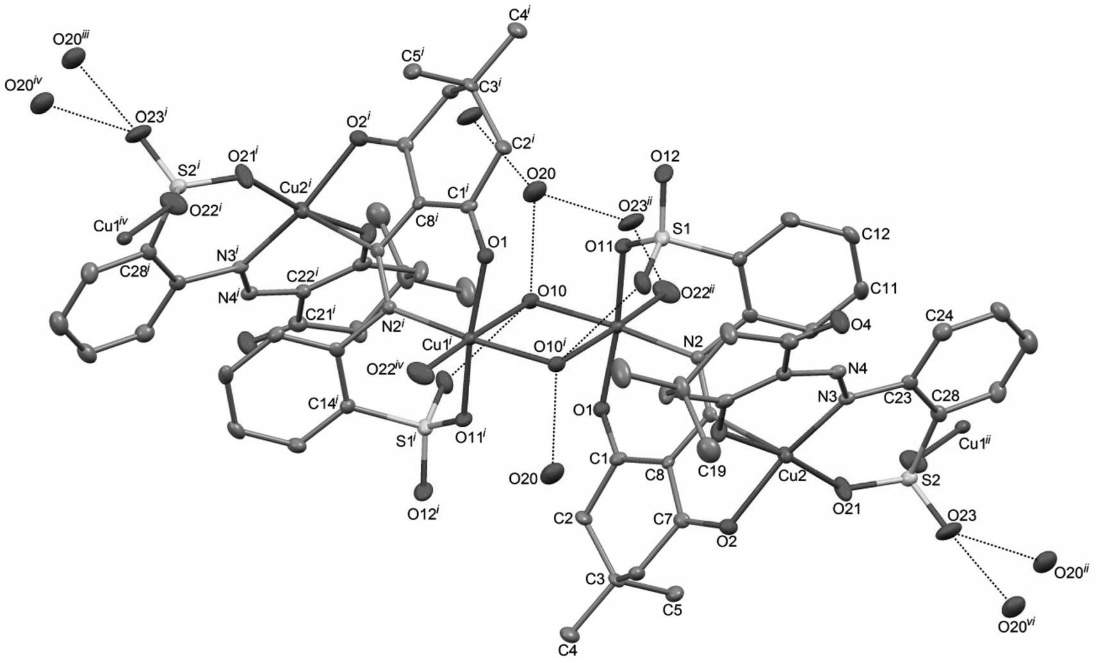

Figure 2. Molecular structure of compound **2** with atomic numbering scheme and showing the strongest intermolecular hydrogen-bonding interactions. Thermal ellipsoids are drawn at the 50% probability level. Selected bond lengths [Å] and angles [°]: N1–N2 1.283(4), N1–Cu2 2.448(3), N2–Cu1 1.969(3), N3–N4 1.295(4), O1–Cu1 1.925(2); O1–Cu1–O11 171.46(10), O1–Cu1–N2 89.22(11), O11–Cu1–N2 93.14(11), O1–Cu1–O10 89.32(10), O11–Cu1–O10 87.26(10), N2–Cu1–O10 172.46(11). Selected hydrogen bonds {*d*(H···A) [Å], ∠(DHA) [°]}: O10–H10A···O13i 1.832(2), 147.41(16); O10–H1OB···O20 1.667(3), 175.53(17); O20–H20C···O23 1.957(3), 167.09(19); O20–H20D···O23 1.991(3), 154.76(18). Symmetry operations to generate equivalent atoms: (i) –*x*, 1 – *y*, 1 – *z*; (ii) 1 – *x*, 1 – *y*, 1 – *z*; (iii) –1 – *x*, –*y*, 1 – *z*; (iv) –1 + *x*, *y*, *z*; (v) –1 + *x*, –1 + *y*, *z*; (vi) 1 + *x*, 1 + *y*, *z*.

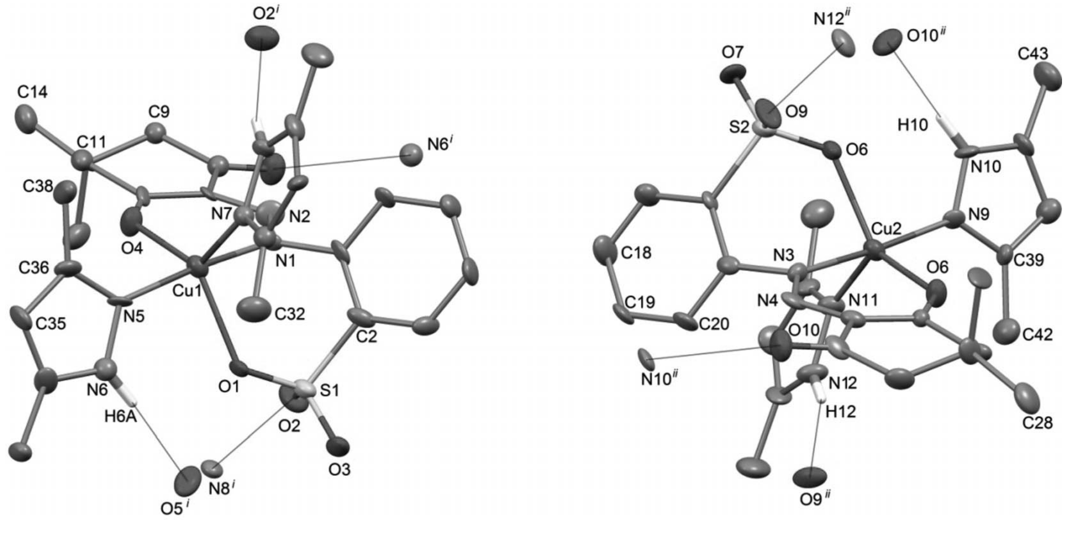

Figure 3. Molecular structure of compound **3** with atomic numbering scheme and showing the intra- as well as the strongest intermolecular hydrogen-bonding interactions. Thermal ellipsoids are drawn at the 50% probability level. Selected bond lengths [Å] and angles [°]: N1–N2 1.288(9), N1–Cu1 1.946(7), N5–N6 1.373(9), N5–Cu1 1.984(8), N7–N8 1.383(9), N7–Cu1 2.084(7), O1–Cu1 2.138(6), O4–Cu1 1.965(6); N1–Cu1–N5 172.7(3), O4–Cu1–N7 122.5(3), N5–Cu1–N7 94.2(3), O4–Cu1–O1 133.0(3). Selected hydrogen bonds {*d*(H···A) [Å], ∠(DHA) [°]}: N6–H6A···O5 2.45, 119.7; N8–H8···O2 2.00, 158.4; N10–H10···O10 2.37, 121.9; N12–H12···O9 1.98, 156.2. Symmetry operations to generate equivalent atoms: (i) 1.5 – *x*, ½ + *y*, ½ – *z*; (ii) ½ – *x*, –½ + *y*, ½ – *z*.

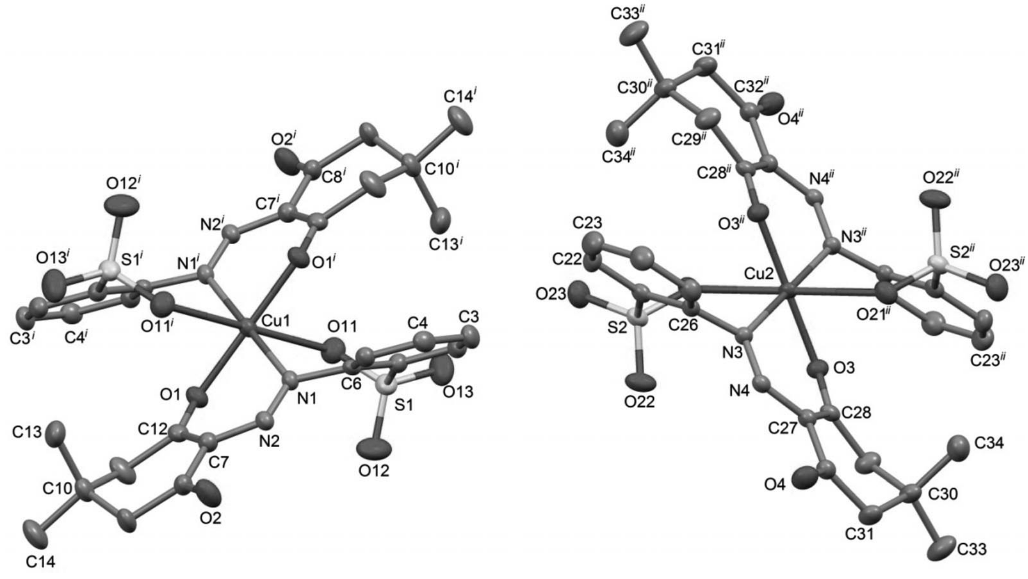

Figure 4. Molecular structure of the complex dianions of **4** with atomic numbering scheme. Thermal ellipsoids are drawn at the 50% probability level. Selected bond lengths [Å] and angles [°]: N1–N2 1.275(3), C6–N1 1.433(4), C7–N2 1.366(4), N3–N4 1.280(3), N1–Cu1 1.968(2), O1–Cu1 1.954(2), O11–Cu1 2.421(2); N2–N1–C6 113.0(2), O1–Cu1–N1 87.46(9), O1–Cu1–O11 97.33(9), N1–Cu1–O11 84.66(8), N1–N2–C7 120.2(2), N4–N3–C26 114.1(2). Symmetry operations to generate equivalent atoms: (i) 1 – *x*, –*y*, –*z*: (ii) –*x*, 1 – *y*, 1 – *z*.

The Cu1 cations form edge-sharing bi-octahedrons each with two bridging aqua ligands, the two distorted octahedra dividing the common O_{aqua}–$O_{aqua}{}^{i}$ edge. The anionic L^{2-} ligand acts as a tridentate O,N,O ligand to Cu1 and, simultaneously, as a N,O ligand to the pentacoordinate Cu2. Consequently, complex **2** is the first metal–AHDB complex in which both nitrogen atoms of the hydrazone unit are effectively coordinated to a metal cation. Moreover, the pentacoordinate L^{2-} ligand displays the major distortion found in these complexes, whereas the ligand coordinated solely to Cu2 is considerably more planar, which is evidenced by the angle between the C and Ar planes [66.52(18) and 21.3(3)°, respectively]. The complexes **3**–**6** (Figures 3, 4, 5 and 6) exhibit intermediate values ranging from 34.7(3) to 61.5(5)°, which substantiates the twisting of the AHBD ligand upon coordination.

Complexes **2** and **4**–**6** illustrate well the influence of the co-ligand in the coordination mode of AHBD (due to its different geometry, complex **3** is excluded from this discussion). Apparently, co-ligand imposed geometry constrictions oblige the $O_{carbonyl}$ and N atoms from the hydrazone molecule to occupy equatorial positions and its $O_{sulfonate}$ atom to occupy the apical site, as observed in structures **4** (with two AHBD ligands) and **5** (with 2,2′-bipyridine). In contrast, for **2** and **6**, in which ligand constraints are less evident, the $O_{carbonyl}$, the N and the $O_{sulfonate}$ atoms of the hydrazone occupy the equatorial positions.

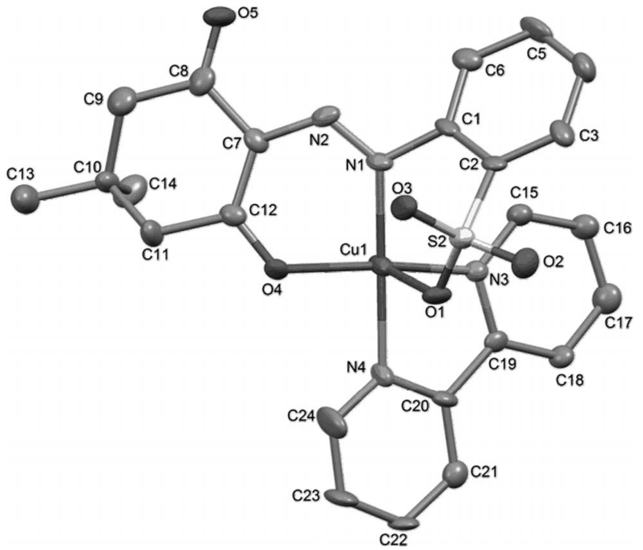

Figure 5. Molecular structure of complex **5** with atomic numbering scheme. Thermal ellipsoids are drawn at the 50% probability level. Selected bond lengths [Å] and angles [°]: C1–N1 1.437(7), C7–N2 1.357(7), N1–N2 1.283(6), N1–Cu1 1.980(4), N3–Cu1 2.037(4), N4–Cu1 2.003(4), O1–Cu1 2.255(4), O4–Cu1 1.943(4); N1–Cu1–N4 172.1(2), O4–Cu1–N3 159.26(17), N1–Cu1–N3 102.56(18), N4–Cu1–N3 81.60(18), O4–Cu1–O1 104.86(15), N4–Cu1–O1 84.61(17), N3–Cu1–O1 93.59(16).

In complexes **2**–**6** (Figures 2–6), the ligand **1** presents two different coordination modes and the copper ion features diverse coordination numbers and geometries. It is in the 2D polymer **2** that the L^{2-} moiety presents the most intricate coordination mode sharing three oxygen and two nitrogen atoms with two copper cations in a $1\kappa^{2}O,\kappa N{:}2\kappa O,\kappa N$ manner. In the other complexes the ligand acts as a $\kappa^{2}O,\kappa N$ donor. The copper cations adopt a distorted octahedral (**2**), a trigonal bipyramid (**3**), a perfect octahedral (**4**) or a square pyramid (**5** and **6**) geometry. Addison and Reedijk and co-workers[11] introduced a parameter (τ_5) to describe the geometry of a five-coordinate metal system, which is determined by Equation (1) in which β and α are the largest angles involving the metal. By means of this simple criterion, perfect square-pyramid or trigonal-bipyramid geome-

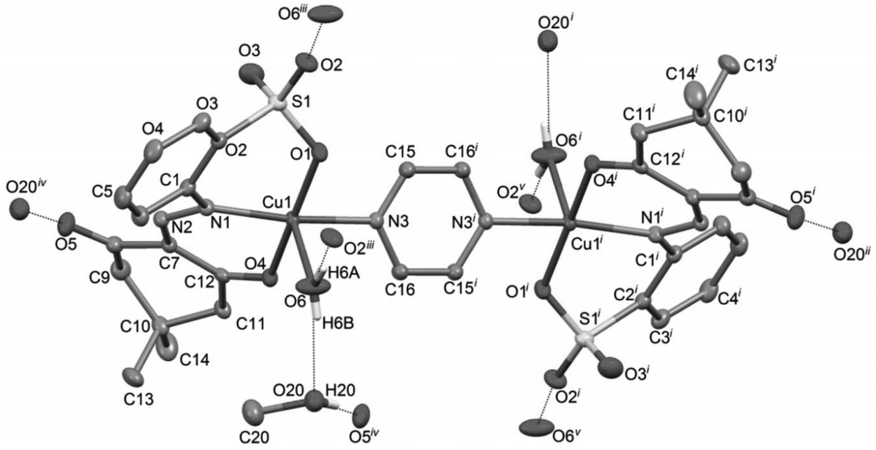

Figure 6. Molecular structure of complex **6** with atomic numbering scheme. Thermal ellipsoids are drawn at the 50% probability level. Selected bond lengths [Å] and angles [°]: N1–N2 1.2810(18), N1–Cu1 1.9767(13), N3–Cu1 2.0235(13), O4–Cu1 1.9240(11), O6–Cu1 2.1690(14); N2–N1–Cu1 127.12(10), O4–Cu1–O1 171.22(5), N1–Cu1–N3 166.79(5), O4–Cu1–N1 88.81(5), O4–Cu1–N3 87.61(5). Selected hydrogen bonds {d(H···A) [Å], ∠(DHA) [°]}: O6–H6A···O2 1.93, 168.5; O6–H6B···O20 2.05(2), 166(3); O20–H20···O5 2.03, 162.9. Symmetry operations to generate equivalent atoms: (i) $-x, -y, 1-z$; (ii) $-1+x, -y, 1-z$; (iii) $1-x, -y, 1-z$; (iv) $-1+x, y, z$; (v) $-1+x, -1+y, z$.

tries should have τ_5 values of 0 or 1, respectively. The τ_5 values for our complexes with a pentacoordinate copper centre are listed in Table 1. Complexes **2** and **6** have τ_5 values very close to zero (0.08 and 0.07, respectively), which fit a square-pyramid geometry. Complex **3**, with τ_5 values of 0.67 and 0.63, support the assignment of a distorted trigonal-bipyramidal geometry. The value of τ_5 for complex **5** (0.21) indicates its immediacy to the square-pyramidal geometry.

$$\tau_5 = (\beta - \alpha)/60° \qquad (1)$$

The crystal lattices in **2**, **3** and **6** are stabilized by medium-to-strong intermolecular hydrogen-bonding interactions (Figures 2, 3 and 6) between the free water molecule and the sulfonate or bridging water molecules (**2**), the N atom of the pyrazolyl and the *O*-sulfonate (**3**) and the free methanol molecule and the coordinated water or sulfonate moieties (**6**).

Catalytic Activity of 2–6 in Cyclohexene Oxidation

Complexes **2**–**6** were tested as catalysts for the selective mild peroxidative oxidation (with TBHP) of cyclohexene to cyclohex-2-enol and cyclohex-2-enone (Scheme 1). The amount of oxidant, reaction time and temperature were varied to optimize the yields of the desired products (Table 2, Figures S2 and S3 in the Supporting Information). The results show that it is possible to obtain a good molar ratio (9–10) of the products (entries 5, 8 and 10) with yields of up to around 70% and TONs of up to 350 (entry 8). Increasing the temperature (from 298 to 328 K) led to improved yields and TONs (Table 2, Figure S2 for catalyst **5**) and under similar conditions, at 328 K, the activities of all the complexes are comparable (entries 2, 4, 6 and 8). Nevertheless, the highest yield and TON were achieved for the pentacoordinate complex **5** (entry 8), a possible precursor of an eventual less sterically hindered active metal centre under the reaction conditions.

Table 2. Peroxidative oxidation of cyclohexene to cyclohex-2-enol and cyclohex-2-enone.[a]

Entry	Catalyst	T [K]	Ketone/ alcohol[b]	Yield [%][c]	TON[d] (TOF)[e]
1	**2**	298	1.1	15.2	30 (3.7)
2	**2**	328	6.7	66.3	330 (13.7)
3	**3**	298	4.0	15.0	30 (3.7)
4	**3**	328	5.7	65.2	325 (13.5)
5	**4**	298	9.0	20.2	40 (2.5)
6	**4**	328	3.5	53.4	265 (11.0)
7	**5**	298	4.0	24.8	50 (6.2)
8	**5**	328	9.0	70.3	350 (14.6)
9[f]	**6**	298	–	–	–
10	**6**	328	10.1	44.9	225 (9.4)
11	blank	298 or 328	–	–	–
12	$Cu(CH_3COO)_2$	328	4.0	32.4	–
13	**1**	328	–	–	–
14[g]	Cu–A	323	3.4	79	(18.2)
15[h]	B	393	–	51	–
16[i]	C	323	2.1	–	31
17[j]	D	353	0.1	4	–

[a] Selected data are presented. Reaction conditions (unless stated otherwise): C_6H_{10} (2.0 mmol at 298 K and 5.0 mmol at 328 K), MeCN (5 mL), catalyst precursor (0.01 mmol), TBHP (5 mmol added as a 70% aqueous solution). The data in entries 14–17 are taken from the literature and are included for comparative purposes. [b] Product molar ratio. [c] Moles of products/100 mol of C_6H_{10}. [d] Overall TON values (mol of products/mol of catalyst). [e] TOF = TON/h (values are given in parentheses) at 298 and 328 K for reaction times of 8 and 24 h, respectively. [f] Products are negligible. [g] Cu catalyst immobilized on modified silica, A = *N*-(hydroxyphenyl)salicyldimine; ketone/epoxide = 19; see ref.[8a] [h] B = calcined (Cr)MCM-48 (MCM-48 = molecular sieves). Alcohol was not observed; ketone/epoxide = 5.0 and ketone/1,2-cyclohexanediol = 11; see ref.[8b] [i] Cu–MOF (metal–organic framework), C = $[Cu(BF_4)_2(OH_2\cdots bpy)(bpy)]$, bpy = 4,4′-bipyridine. Ketone/2-cyclohexene hydroperoxide = 0.07 and ketone/epoxide = 2.9; see ref.[8e] [j] D = α-titanium–Cu–arsenate/TBHP; ketone/epoxide = 0.05; see ref.[8f]

Another important factor in the performance of the system concerns the relative amount of TBHP oxidant. An increase in the peroxide-to-catalyst molar ratio results in an increase in the yield (Figure S3 for catalyst **5**), for example, from around 57 to 70% (24 h reaction time) upon changing the ratio from 0.5 to 1.5 at 328 K.

Many metal complexes have been used as catalysts or catalyst precursors for the peroxidative oxidation of cyclohexene in homogeneous and heterogeneous catalysis,[8] such as those quoted in entries 14–17 of Table 2 for comparative purposes. Some Cu–Schiff base complexes can lead to a higher yield (79%) of products (entry 14),[8a] whereas a heterogeneous chromium species leads to a yield (51%; entry 15)[8b] that is lower than those (ca. 65–70%) we observed for **2**, **3** and **5**. However, these catalysts show lower selectivities than our systems, leading to lower ketone/alcohol molar ratios and also to epoxide formation. Various products were also observed when the Cu–MOF (metal–organic framework) $[Cu(BF_4)_2(OH_2\cdots bpy)(bpy)]$ (bpy = 4,4′-bipyridine) and α-titanium–Cu–arsenate were used as catalysts, the main ones being 2-cyclohexene hydroperoxide and the epoxide, respectively (Table 2, entries 16 and 17).[8e,8f] Therefore our complex **5** (Table 2, entry 8) is among the best catalyst precursors for selective allylic cyclohexene oxidation, which results in the preferred formation of the ketone.

Conclusions

A new water-soluble AHBD functionalized with a sulfonic acid group has been synthesized and fully characterized by elemental analysis, IR, ^1H and ^{13}C NMR spectroscopy and single-crystal X-ray analysis. It has been shown that it acts as a versatile ligand, forming new water-soluble Cu^{II}–AHBD complexes of different nuclearities and diverse structures simply by treating copper acetate with AHBD in the absence or presence of a coordinating N species such as 3,5-dimethyl-1*H*-pyrazole, cyanoguanidine, 2,2′-bipyridine or pyrazine. Their structural diversity is reflected in the important roles played by AHBD and the auxiliary ligands in the assembly of the resulting frameworks. Thus, the tuneable synthesis of a variety of complexes of different geometries and nuclearities by a simple and convenient method has been achieved.

The thus synthesized water-soluble Cu^{II}–AHBD complexes can be used as efficient and selective catalysts for the peroxidative oxidation of cyclohexene to cyclohex-2-enol and cyclohex-2-enone under mild conditions to give good yields and TONs. This approach deserves further exploration in the search for other types of functionalized water-soluble AHBD ligands and metal ions.

Experimental Section

Materials and Instrumentation: The ^1H and ^{13}C NMR spectra were recorded at room temperature with a Bruker Avance II + 300 (UltraShield™ Magnet) spectrometer operating at 300.130 and 75.468 MHz for ^1H and ^{13}C NMR, respectively. The chemical shifts are reported in ppm with tetramethylsilane as the internal reference. IR spectra (4000–400 cm^{-1}) were recorded with a BIO-RAD FTS 3000MX instrument in KBr pellets. CHN elemental analyses were carried out at the Microanalytical Service of the Instituto Superior Técnico. All the synthetic work was performed in air at room temperature. Chromatographic analyses were undertaken by using a Fisons Instruments GC 8000 series gas chromatograph with a DB-624 (J&W) capillary column (FID detector) and the Jasco-Borwin v.1.50 software. The organic products were quantified by the internal standard method; calibration curves with estimated errors are given in Figure S4.

2-[2-(4,4-Dimethyl-2,6-dioxocyclohexylidene)hydrazinyl]benzenesulfonic Acid (1): Compound **1** was synthesized by a modified[9d] Japp–Klingemann reaction[9a–9c] between the aromatic diazonium salt of 2-sulfoaniline and 5,5-dimethylcyclohexane-1,3-dione in water solution containing sodium hydroxide.

Diazotization: 2-Sulfoaniline (4.325 g, 25 mmol) was dissolved in water (50 mL) and NaOH (0.50 g, 12.5 mmol) was added. The solution was cooled in an ice bath to 273 K and $NaNO_2$ (1.725 g, 25 mmol) was added. HCl (5.00 mL) was then added in 0.5 mL portions over 1 h. The temperature of the mixture should not exceed 278 K.

Azocoupling: NaOH (1.00 g, 25 mmol) was added to a mixture of 5,5-dimethylcyclohexane-1,3-dione (3.50 g, 25 mmol) in ethanol (50 mL). The solution was cooled in an ice bath to around 273 K and a suspension of 2-sulfoaniline diazonium chloride (see above) was added in three portions under vigorous stirring over 1 h. The precipitated yellow product was filtered off, dried in air and recrystallized from ethanol to give crystals of suitable quality for X-ray analysis.

H_2L^1 (1): Yield: 77% (based on 5,5-dimethylcyclohexane-1,3-dione), yellow powder soluble in water, methanol, ethanol, acetone and insoluble in chloroform. IR (KBr): $\tilde{\nu}$ = 3491 (νOH), 2954 (νNH), 1664 (νC=O), 1630 (νC=O···H), 1578 (νC=N) cm^{-1}. ^1H NMR (300.130 MHz, [D$_6$]DMSO, internal TMS): δ = 0.98 (3 H, CH_3), 1.02 (3 H, CH_3), 2.56 (2 H, CH_2), 2.60 (2 H, CH_2), 7.17–7.84 (4 H, Ar–H), 15.28 (1 H, NH) ppm. $^{13}C\{^1H\}$ NMR (75.468 MHz, [D$_6$]DMSO, internal TMS): δ = 28.1 (CH_3), 30.3 (CH_3), 46.0 (C_{ipso}), 51.8 (CH_2), 52.2 (CH_2), 116.4 (Ar-H), 125.3 (Ar-H), 127.5 (Ar-H), 130.6 (Ar-H), 130.7 (Ar-SO_3H), 136.1 (C=N), 138.4 (Ar-NH-N), 193.3 (C=O), 195.2 (C=O) ppm. $C_{14}H_{16}N_2O_5S$ (324): calcd. C 51.72, H 4.48, N 8.53; found C 51.84, H 4.97, N 8.64.

Synthesis of Copper(II) Complexes 2–6: Compound **1** (1 mmol) was dissolved in water (30 mL) and then $Cu(CH_3COO)_2\cdot H_2O$ (1 mmol) and (in the cases of **3**–**6**, 1 mmol of) 3,5-dimethyl-1*H*-pyrazole (dp), cyanoguanidine (cyg), 2,2′-bipyridine (bpy) or pyrazine (py), respectively, were added. The mixture was stirred at reflux for 15 min and left to slowly evaporate. After evaporation of the solvent, the microcrystalline product was recrystallized from methanol and water (2:1, v/v). All the complexes are soluble in water, methanol, ethanol and DMSO.

2: Yield: 54% (based on Cu). IR (KBr): $\tilde{\nu}$ = 3536 (br. s, νOH), 1674 (s) (νC=O), 1621 δ(OH, H_2O), 1602 (s) (νC=N) cm^{-1}. $C_{28}H_{32}Cu_2N_4O_{12}S_2$ (807.8): calcd. C 41.63, H 3.99, N 7.54; found C 41.32, H 3.73, N 7.46.

3: Yield: 63% (based on Cu). IR (KBr): $\tilde{\nu}$ = 2360 (br. s, νNH), 1637 (s, νC=O), 1528 (s, νC=N) cm^{-1}. $C_{24}H_{30}CuN_6O_5S$ (578.1): calcd. C 49.86, H 5.23, N 14.54; found C 49.67, H 5.13, N 14.45.

Table 3. Crystal data and structure refinement details for compounds **1**–**6**.

	1	**2**	**3**	**4**	**5**	**6**
Formula unit	$C_{14}H_{15}N_2O_5S$	$C_{28}H_{32}Cu_2N_4O_{12}S_2$	$C_{24}H_{30}CuN_6O_5S$	$C_{28}H_{28}CuN_4O_{10}S_2$	$C_{24}H_{22}CuN_4O_5S$	$C_{34}H_{44}Cu_2N_6O_{14}S_2$
Formula mass	323.34	807.78	578.14	708.20	542.06	951.95
Crystal system	orthorhombic	triclinic	monoclinic	triclinic	monoclinic	triclinic
Space group	*P*212121	$P\bar{1}$	*P*21/*n*	$P\bar{1}$	*P*21/c	$P\bar{1}$
a [Å]	6.4413(2)	11.2517(4)	19.480(2)	10.0268(3)	11.0281(12)	7.7982(2)
b [Å]	14.9502(5)	11.3996(3)	12.3303(14)	12.5244(4)	27.196(3)	9.5126(2)
c [Å]	19.9725(6)	13.4223(5)	23.349(3)	16.2570(6)	8.6830(9)	13.4944(3)
α [°]	90.00	113.166(3)	90.00	69.3980(10)	90.00	91.5850(10)
B [°]	90.00	91.521(2)	112.211(5)	80.837(2)	92.217(4)	93.436(2)
γ [°]	90.00	101.5220(10)	90.00	80.9000(10)	90.00	101.1300(10)
Z	4	2	8	2	4	1
Volume [Å^3]	1923.33(11)	1540.30(9)	5192.2(11)	1875.05(11)	2602.2(5)	979.65(4)
D_c [g cm^{-3}]	1.117	1.742	1.479	1.254	1.384	1.614
μ(Mo-K_α) [mm^{-1}]	0.188	1.589	0.969	0.745	0.960	1.267
Reflections collected	12817	22226	35389	18854	19701	24151
Unique reflections	4148	6314	9482	6823	5724	6528
R_{int}	0.0592	0.0712	0.3189	0.0317	0.1470	0.0379
Final *R*1,[a] *wR*2[b] ($I \geq 2\sigma$)	0.0916, 0.2459	0.0420, 0.0983	0.0763, 0.0937	0.0454, 0.1308	0.0664, 0.1636	0.0314, 0.0752
GOF on F^2	1.078	1.015	0.886	1.058	0.838	0.983

[a] $R1 = \Sigma||F_o| - |F_c||/\Sigma|F_o|$. [b] $wR2 = \{\Sigma[w(F_o^2 - F_c^2)^2]/\Sigma[w(F_o^2)^2]\}^{1/2}$.

4: Yield: 61% (based on Cu). IR (KBr): ṽ = 3343 (br. s, νOH), 1655 (s, νC=O), 1630 (δOH, H_3O^+), 1553 (s, νC=N) cm^{-1}. $C_{28}H_{34}CuN_4O_{12}S_2$ (746.26): calcd. C 45.06, H 4.59, N 7.51; found C 45.01, H 4.52, N 7.54.

5: Yield: 53% (based on Cu). IR (KBr): ṽ = 1637 (s, νC=O), 1601 (s, νC=O), 1535 (s, νC=N) cm^{-1}. $C_{24}H_{22}CuN_4O_5S$ (542.1): calcd. C 53.18, H 4.09, N 10.34; found C 53.23, H 4.45, N 10.47.

6: Yield: 56% (based on Cu). IR (KBr): ṽ = 3220 (br. s, νOH), 1658 (s, νC=O), 1632 (δOH, H_2O), 1509 (s, νC=N) cm^{-1}. $C_{33}H_{40}Cu_2N_6O_{13}S_2$ (919.9): calcd. C 43.09, H 4.38, N 9.14; found C 43.05, H 4.21, N 9.08.

X-ray Structure Determinations: X-ray quality single-crystals of complexes **1**–**6** were immersed in cryo-oil, mounted in a Nylon loop and measured at a temperature of 150 K (Table 3). Intensity data were collected by using a Bruker AXS-KAPPA APEX II diffractometer with graphite-monochromated Mo-K_α (λ = 0.71073) radiation. Data were collected by using ω scans of 0.5° per frame and a full sphere of data were obtained. Cell parameters were retrieved by using the Bruker SMART software and refined by using Bruker SAINT[12a] on all the observed reflections. Absorption corrections were applied by using the SADABS software.[12b] The structures were solved by direct methods by using the SHELXS-97 package[12c] and refined with SHELXL-97.[12d] Calculations were performed by using the WinGX System Version 1.80.03.[12b] All hydrogen atoms were inserted at calculated positions. Least-squares refinements with anisotropic thermal motion parameters for all the non-hydrogen atoms and isotropic parameters for the remaining atoms were employed. Disordered solvents were present in the structures of complexes **1**, **4** and **5**. Because no obvious major site occupations were found for those molecules, it was not possible to model them. PLATON/SQUEEZE[12d] was used to correct the data and potential volumes of 483.3 (for **1**), 463.7 (for **4**) and 434.0 (for **5**) Å^3 were found with, respectively, 217, 148 and 190 electrons per unit cell worth of scattering. The electron counts suggest the presence of around two molecules of ethanol (for **1**), around two molecules of water (for **4**) and around one molecule of methanol and one molecule of water (for **5**) per unit cell. The modified datasets improved the *R*1 factor markedly. To accomplish charge equilibrium in the structure of **4**, we believe the disordered water molecules are protonated.

CCDC-850011 (for **1**), -850012 (for **2**), -850013 (for **3**), -850014 (for **4**), -850015 (for **5**) and -850016 (for **6**) contain the supplementary crystallographic data for this paper. These data can be obtained free of charge from The Cambridge Crystallographic Data Centre via www.ccdc.cam.ac.uk/data_request/cif.

Oxidation of Cyclohexene: The reaction mixtures were prepared as follows: MeCN (5.0 mL), C_6H_{10} (2.00–5.00 mmol) and TBHP (70% solution in H_2O, 2.50–7.50 mmol), in this order, were added to complex **2**–**6** (0.010 mmol) in a reaction flask. The reaction mixture was stirred for the required time, typically 8 h, at room temperature (ca. 298 K) or for 24 h at 338 K in air. Then cyclooctane (10 µL, as internal standard) and diethyl ether (2.0 mL, to extract the substrate and the products from the reaction mixture) were added. The resulting mixture was stirred for 15 min and then a sample taken from the organic phase was analysed by GC. Blank experiments were performed and confirmed that no cyclohexene oxidation products were formed in the absence of the metal catalyst.

Supporting Information (see footnote on the first page of this article): Packing diagrams of compound **2**, effects of temperature and TBHP/C_6H_{10} molar ratio on the overall yield of cyclohex-2-enol and cyclohex-2-enone, calibration curves for determination of cyclohexene-1-one and cylohexene-2-ol.

Acknowledgments

This work was partially supported by the Fundação do Ministério de Ciência e Tecnologia (FCT) (project numbers PTDC/QUI-QUI/102150/2008 and PEst-OE/QUI/UI0100/2011) and "Science" programs. The authors acknowledge the Portuguese NMR Network for providing access to the NMR facility.

---

[1] E. V. Shchegol'kov, Y. V. Burgart, O. G. Khudina, V. I. Saloutin, O. N. Chupakhin, *Russ. Chem. Rev.* **2010**, *79*, 31–61.

[2] a) M. N. Kopylovich, K. T. Mahmudov, M. F. C. Guedes da Silva, M. L. Kuznetsov, P. J. Figiel, Y. Y. Karabach,

K. V. Luzyanin, A. J. L. Pombeiro, *Inorg. Chem.* **2011**, *50*, 918–931; b) J. Marten, W. Seichter, E. Weber, *Z. Anorg. Allg. Chem.* **2005**, *631*, 869–877; c) E. Weber, J. Marten, W. Seichter, *J. Coord. Chem.* **2009**, *62*, 3401–3410; d) A. M. Maharramov, R. A. Aliyeva, K. T. Mahmudov, A. V. Kurbanov, R. K. Askerov, *Russ. J. Coord. Chem.* **2009**, *35*, 704–709; e) M. N. Kopylovich, K. T. Mahmudov, M. Haukka, K. V. Luzyanin, A. J. L. Pombeiro, *Inorg. Chim. Acta* **2011**, *374*, 175–180.

[3] a) P. Gilli, V. Bertolasi, V. Ferretti, G. Gilli, *J. Am. Chem. Soc.* **2000**, *122*, 10405–10417; b) P. Gilli, V. Bertolasi, L. Pretto, A. Lycka, G. Gilli, *J. Am. Chem. Soc.* **2002**, *124*, 13554–13567; c) P. Gilli, V. Bertolasi, L. Pretto, G. Gilli, *J. Mol. Struct.* **2006**, *790*, 40–49.

[4] a) J. McVie, D. Alastair, R. S. Sinclair, T. G. Truscott, *J. Chem. Soc. Perkin Trans. 2* **1980**, 286–290; b) J. Marten, A. Erbe, K. Critchley, J. P. Bramble, E. Weber, S. D. Evans, *Langmuir* **2008**, *24*, 2479–2486; c) M. J. Jeong, J. H. Park, C. Lee, J. Y. Chang, *Org. Lett.* **2006**, *8*, 2221–2224; d) W. Malik, R. N. Goyal, V. K. Mahest, *Electroanal. Chem.* **1975**, *62*, 451–458; e) H. B. Hassib, Y. M. Issa, W. S. Mohamed, *J. Therm. Anal. Calorim.* **2008**, *92*, 775–782; f) M. N. Kopylovich, K. T. Mahmudov, A. J. L. Pombeiro, *J. Hazard. Mater.* **2011**, *186*, 1154–1162; g) T. Ishizuki, H. Wada, G. Nakagawa, *Anal. Chim. Acta* **1988**, *212*, 253–260; h) K. T. Mahmudov, R. A. Aliyeva, S. R. Gadjieva, F. M. Chyragov, *J. Anal. Chem.* **2008**, *63*, 435–438; i) K. T. Mahmudov, A. M. Maharramov, R. A. Aliyeva, I. A. Aliyev, M. N. Kopylovich, A. J. L. Pombeiro, *Anal. Lett.* **2010**, *43*, 2923–2938; j) K. T. Mahmudov, M. N. Kopylovich, M. F. C. G. Guedes da Silva, P. J. Figiel, Y. Y. Karabach, A. J. L. Pombeiro, *J. Mol. Catal. A* **2010**, *318*, 44–50; k) M. N. Kopylovich, A. C. C. Nunes, K. T. Mahmudov, M. Haukka, T. C. O. Mac Leod, L. M. D. R. S. Martins, M. L. Kuznetsov, A. J. L. Pombeiro, *Dalton Trans.* **2011**, *40*, 2822–2836; l) M. N. Kopylovich, T. C. O. Mac Leod, K. T. Mahmudov, M. F. C. G. Guedes da Silva, A. J. L. Pombeiro, *Dalton Trans.* **2011**, *40*, 5352–5361; m) J. Sokolnicki, J. Legendziewicz, W. Amirkhanov, V. Ovchinnikov, L. Macalik, J. Hanuza, *Spec. Chim. Acta Part A* **1999**, *55*, 349–367; n) F. Huang, Y. Wu, D. Gu, F. Gan, *Thin Solid Films* **2005**, *483*, 251–256; o) Z. Chen, F. Huang, Y. Wu, D. Gu, F. Gan, *Inorg. Chem. Commun.* **2006**, *9*, 21–24.

[5] M. N. Kopylovich, K. T. Mahmudov, M. Haukka, P. J. Figiel, M. Archana, J. A. L. da Silva, A. J. L. Pombeiro, *Eur. J. Inorg. Chem.* **2011**, *27*, 4175–4181.

[6] a) A. S. de Sousa, M. A. Fernandes, K. Padayachy, H. M. Marques, *Inorg. Chem.* **2010**, *49*, 8003–8011; b) H. Lin, H. Hu, X. Wang, B. Mu, J. Li, *J. Coord. Chem.* **2010**, *63*, 1295–1303; c) J. W. Steed, D. R. Turner, K. J. Wallace, *Core Concepts in Supramolecular Chemistry and Nanochemistry*, Wiley, Chichester, New York, **2007**.

[7] a) E. R. T. Tieking, J. Vittal (Eds.), *Frontiers in Crystal Engineering*, Wiley, Hoboken, NY, **2006**; b) E. Weber, in: *Kirk Othmer Encyclopedia of Chemical Technology* (Ed.: J. I. Kroschwitz), 4th ed., Wiley, New York, **1998**, Suppl., pp. 352–396; c) H.-J. Schneider, A. Yatsimirsky, *Principles and Methods in Supramolecular Chemistry*, Wiley, Chichester, New York, **2000**; d) D. D. MacNicol, S. J. Rowan, in: *Comprehensive Supramolecular Chemistry* (Eds.: J. L. Atwood, J. E. D. Davies, D. D. MacNicol, F. Vögtle), Elsevier, Oxford, UK, **1996**, vol. 10, pp. 417–428; e) T. Hertzsch, J. Hulliger, E. Weber, P. Sozzani, in: *Encyclopedia of Supramolecular Chemistry* (Eds.: J. L. Atwood, J. W. Steed), CRC Press, Boca Raton, FL, **2004**, pp. 996–1005; f) J. Janata, *Chem. Rev.* **2008**, *108*, 327–328.

[8] a) S. Mukherjee, S. Samanta, B. C. Roy, A. Bhaumik, *Appl. Catal. A* **2006**, *301*, 79–88; b) A. Sakthivel, S. E. Dapurkar, P. Selvam, *Appl. Catal. A* **2003**, *246*, 283–293; c) M. B. Meder, L. H. Gade, *Eur. J. Inorg. Chem.* **2004**, 2716–2722; d) E. F. Murphy, T. Mallat, A. Baiker, *Catal. Today* **2000**, *57*, 115–126; e) D. Jiang, T. Mallat, D. M. Meier, A. Urakawa, A. Baiker, *J. Catal.* **2010**, *270*, 26–33; f) S. Khar, S. Shrivastava, *J. Mol. Catal. A* **2004**, *217*, 51–58; g) C. Adhikary, R. Bera, B. Dutta, S. Jana, G. Bocelli, A. Cantoni, S. Chaudhuri, S. Koner, *Polyhedron* **2008**, *27*, 1556–1562; h) S. Jana, B. Dutta, R. Bera, S. Koner, *Langmuir* **2007**, *23*, 2492–2496; i) B. Dutta, S. Jana, R. Bera, P. K. Saha, S. Koner, *Appl. Catal. A* **2007**, *318*, 89–94.

[9] a) F. R. Japp, F. Klingemann, *Justus Liebigs Ann. Chem.* **1888**, *247*, 190–220; b) H. C. Yao, P. Resnick, *J. Am. Chem. Soc.* **1962**, *84*, 3514–3517; c) H. C. Yao, *J. Org. Chem.* **1964**, *29*, 2959–2963; d) M. N. Kopylovich, K. T. Mahmudov, M. F. C. G. Silva, L. M. D. R. S. Martins, M. L. Kuznetsov, T. F. S. Silva, J. J. R. F. Silva, A. J. L. Pombeiro, *J. Phys. Org. Chem.* **2011**, *24*, 764–773.

[10] F. H. Allen, O. Kennard, D. G. Watson, L. Brammer, A. G. Orpen, R. Taylor, *J. Chem. Soc. Perkin Trans. 2* **1987**, S1–S19.

[11] A. W. Addison, T. N. Rao, J. Reedijk, J. Van Rijn, G. C. Verschoor, *J. Chem. Soc., Dalton Trans.* **1984**, 1349–1356.

[12] a) *APEX2*, *SAINT*, version 6.0, Bruker AXS Inc., Madison, WI, **2004**; b) L. J. Farrugia, *J. Appl. Crystallogr.* **1999**, *32*, 837–838; c) G. M. Sheldrick, *Acta Crystallogr., Sect. A* **2008**, *64*, 112–122; d) A. L. Spek, *Acta Crystallogr., Sect. A* **1990**, *46*, C34.

Received: December 5, 2011